Zeitschrift für Physikalische Chemie Neue Folge, Bd. 118, S. 11–30 (1979)

Photochemical Investigation of the Iodine/Iron System

By

Jürg Baumann, Hans-Rudolf Grüniger and Gion Calzaferri

Institute for Inorganic and Physical Chemistry, University of Bern, Freiestrasse 3, CH-3012 Bern, Switzerland

(Received August 16, 1979)

Photochemistry / Iodine/iron photoredox system / Selective electrodes / Reduction degree

The iodine/iron photoredox system is much more complex than has been assumed up to now. In 0.1 molar sulfuric acid the following reactions have to be considered:

$$
\begin{array}{ll}
(I_2 \text{ or } I_3^-) & \overset{h\nu}{\rightarrow} (I_2 \text{ or } I_3^-)^* \\
(I_2 \text{ or } I_3^-)^* + 2Fe^{2+} & \rightleftarrows (2I^- \text{ resp. } 3I^-) + 2Fe^{3+} \\
2Fe^{3+} + 3I^- & \rightleftarrows 2Fe^{2+} + I_3^- \\
I_2 + I^- & \rightleftarrows I_3^- \\
I_2 \text{ (solid)} & \rightleftarrows I_2 \text{ (solved)} \\
Fe^{3+} + I^- & \rightleftarrows FeI^{2+} \\
Fe^{3+} + SO_4^{2-} & \rightleftarrows FeSO_4^+ \\
Fe^{2+} + SO_4^{2-} & \rightleftarrows FeSO_4
\end{array}
$$

The thermal back reaction $2Fe^{3+} + 3I^- \rightarrow 2Fe^{2+} + I_3^-$ takes several hours. It is therefore possible to separate the electrode compartment and the light absorption measurement cell from the photoreactor. We have built a flow system isolated from air. The following parameters have been measured: light intensity at given spectral distribution, potential of the two selective electrodes versus a reference electrode; light absorption of the solution at constant wavelength, temperature at the electrode surface and electrical current between the two selective electrodes at different external resistances. Using the reduction degree as important degree of freedom it is possible to derive a phenomenological description of the photostationary states of the iodine/iron photoredox system. This phenomenological description provides a good starting point for a more detailed investigation so that it might become possible to understand the primary photoprocesses. The observed quantum yield for the production of Fe^{3+} species lies between 0.05 and 0.58 depending on the composition of the solution.

Das Jod/Eisen-Photoredoxsystem ist wesentlich komplexer als bisher angenommen wurde. Weil die thermische Rückreaktion $2Fe^{3+} + 3I^- \rightarrow 2Fe^{2+} + I_3^-$ sehr langsam abläuft, ist es möglich, den Elektrodenraum und den Ort für die Verfolgung der Lichtabsorption von dem Photoreaktor zu trennen. Wir haben deshalb ein gegen Luft isoliertes Durchfluß-System aufgebaut. Die folgenden Parameter wurden gemessen: Lichtintensität bei gegebener spektra-

ler Verteilung, Potential der beiden selektiven Elektroden gegen eine Referenzelektrode, Lichtabsorption der Lösung bei konstanter Wellenlänge, Temperatur auf der Elektrodenoberfläche und Stromfluß zwischen den beiden selektiven Elektroden bei verschiedenen Außenwiderständen. Durch Verwendung des Reduktionsgrades als wichtigen Freiheitsgrad gelingt es recht gut, photostationäre Zustände des Jod/Eisen-Photoredox-Systems zu beschreiben. Diese phänomenologische Beschreibung bildet eine gute Ausgangslage für detailliertere Untersuchungen, so daß es möglich sein sollte, die Primärprozesse zu verstehen. Die beobachteten Quantenausbeuten liegen zwischen 0,05 und 0,58, je nach Zusammensetzung der Lösung.

1. Introduction

Since more than 50 years it is known [1] that the equilibrium

$$2\,Fe^{3+} + 3\,I^- \rightleftarrows 2\,Fe^{2+} + I_3^- \qquad (A)$$

can be shifted to the left by irradiation with visible light. Electrons are transferred from iron (II) species to energetically excited iodine species:

$$\begin{aligned} (I_2 \text{ or } I_3^-) &\xrightarrow{\text{visible light}} (I_2 \text{ or } I_3^-)^* \\ (I_2 \text{ or } I_3^-)^* + 2\,Fe^{2+} &\longrightarrow (2\,I^- \text{ resp. } 3\,I^-) + 2\,Fe^{3+}. \end{aligned} \qquad (B)$$

Some photochemists have been considering this reaction for solar energy utilization [2, 3]. We have found that the theoretical description and the known experimental data are not sufficient to decide if this system is qualified for the purpose [4]. As soon as selective electrode material for Fe^{3+}/Fe^{2+} and I_2/I^- was found [5, 6], we started a new investigation. We built up an experiment which allowed simultaneous observation of the following quantities: light flux at given spectral distribution, light absorption of the solution as a function of time, temperature in the electrode compartment, potential of the two selective electrodes towards a reference electrode and electrical current between the two electrodes. In order to interpret the experiments, the solubility of the iodine

$$I_2\,(\text{solid}) \rightleftarrows I_2\,(\text{solved}) \qquad (C)$$

and the following complex equilibria had to be considered:

$$\begin{aligned} I_3^- &\rightleftarrows I^- + I_2 \\ FeI^{2+} &\rightleftarrows Fe^{3+} + I^- \\ FeI_2^+ &\rightleftarrows Fe^{3+} + 2\,I^- \\ FeSO_4 &\rightleftarrows Fe^{2+} + SO_4^{2-} \\ FeSO_4^+ &\rightleftarrows Fe^{3+} + SO_4^{2-} \\ Fe(OH)^{2+} &\rightleftarrows Fe^{3+} + OH^- \\ Fe_2(OH)_2^{4+} &\rightleftarrows 2\,Fe^{3+} + 2\,OH^- \end{aligned} \qquad (D)$$

2. Equilibrium and quasistationary states

To describe photoredox systems it is often very useful to know the equilibrium concentration of all species as a function of the reduction degree [5, 7–10]. This provides a good starting point for discussing situations far from equilibrium [5, 10]. We have succeeded in finding a general definition for the reduction degree [10]. Its application leads to:

$$r=\frac{\{[I^-]+[I_3^-]+[FeI^{2+}]+2[FeI_2^+]\}+\{[Fe^{2+}]+[FeSO_4]\}}{I_{tot}+M_0} \qquad (1)$$

I_{tot} is equal to the total iodine concentration:

$$I_{tot}=[I^-]+2[I_2\,(\text{solved})]+3[I_3^-]+[FeI^{2+}]+2[FeI_2^+] +2\cdot I_2\,(\text{solid})\,\frac{1}{V}.$$

The symbol V is used for the total volume. The total concentration on solved iodine species is called I_0:

$$I_0(r)=[I^-]+2[I_2\,(\text{solved})]+3[I_3^-]+[FeI^{2+}]+2[FeI_2^+].$$

At equilibrium I_0 depends on the reduction degree only if $I_0<I_{tot}$. M_0 is equal to the total concentration of iron ions:

$$M_0=[Fe^{3+}]+[FeI^{2+}]+[FeI_2^+]+[Fe^{2+}]+[FeSO_4] +[Fe(OH)^{2+}]+2[Fe_2(OH)_2^{4+}].$$

The reduction degree r is a measure for the number of reduction equivalents which are added to the system in relation to its completely oxidized state. In such a state M_0 equals the concentration of iron(III) species and I_{tot} equals the amount of iodine atoms. The possible values for r lie between 0 and 1. They can be chosen deliberately by weighing or by electrochemical means. The values $r=0$ and $r=1$ can only be reached asymptotically [10]. $r=0$ means that all species are in their oxidized form. $r=1$ means that all species are in their reduced form.

Our experiments have been carried out in 0.1 molar sulfuric acid. In this solution the concentrations of $Fe(OH)^{2+}$ and of $Fe_2(OH)_2^{4+}$ are small so that for most considerations we can neglect them. This does not mean that these complexes are not important for describing kinetics, especially the kinetic at the electrodes [11]. In the used solutions the concentration of FeI_2^+ ions is always small. The equilibria to be considered explicitly are therefore at 25 °C:[1]

$$2Fe^{3+}+3I^- \rightleftarrows 2Fe^{2+}+I_3^- \quad K_1=\ 9.94\cdot 10^7\ \ (\text{l/Mol})^2\ [2]\ [12] \qquad (2.1)$$

[1] in 0.1 molar sulfuric acid the formation of HOI and IO_3^- can be neglected [16]

[2] calculated from standard redox potentials

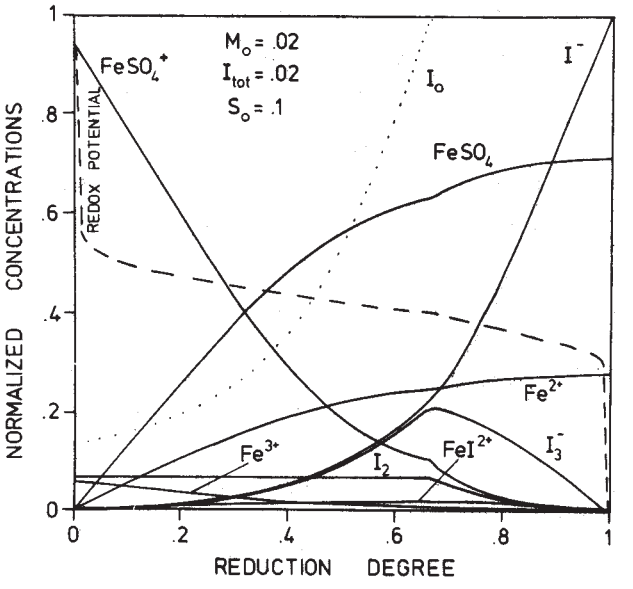

Fig. 1. Normalized equilibrium concentrations and equilibrium redox potential versus the reduction degree. The dotted line corresponds to the total concentration $I_0(r)$ of solved iodine species

$I_2 + I^-$	$\rightleftarrows I_3^-$	$K_2 = 714.3$	l/Mol	[13]	(2.2)
I_2(solid)	$\rightleftarrows I_2$(solved)	$K_3 = 1.34 \cdot 10^{-3}$	Mol/l	[14]	(2.3)
$Fe^{3+} + I^-$	$\rightleftarrows FeI^{2+}$	$K_4 = 708$	l/Mol	[13]	(2.4)
$Fe^{3+} + SO_4^{2-}$	$\rightleftarrows FeSO_4^+$	$K_5 = 204$	l/Mol	[13]	(2.5)
$Fe^{2+} + SO_4^{2-}$	$\rightleftarrows FeSO_4$	$K_6 = 30$	l/Mol^3	[13]	(2.6)

Concentrations of the ten independent species have been calculated with the help of a method described in an earlier paper [15]. Regarding the equilibrium situation, the following four independent conditions are fulfilled:

$$M_0 = [Fe^{3+}] + [Fe^{2+}] + [FeSO_4] + [FeSO_4^+] + (FeI^{2+}) \quad (3.1)$$

$$I_{tot} = [I^-] + 2[I_2(\text{solved})] + 3[I_3^-] + [FeI^{2+}] + 2I_2(\text{solid}) \cdot \frac{1}{V} \quad (3.2)$$

$$r(M_0 + I_{tot}) = \{[I^-] + [I_3^-] + [FeI^{2+}]\} + \{[Fe^{2+}] + [FeSO_4]\} \quad (3.3)$$

$$S_0 = [SO_4^{2-}] + [FeSO_4^+] + [FeSO_4] \quad (3.4)$$

[3] estimated value

These four conditions may be called degrees of freedom, because their values can be chosen deliberately [8, 15]. M_0, I_{tot} and S_0 are used as parameters and r as variable.

If a sample is irradiated at a fixed reduction degree the photoredox reaction takes place – as given by equation (B) – and the individual concentrations are shifted from their equilibrium values. Since no reduction equivalents are supplied to the system, the value of r remains unchanged. Figure 1 gives the normalized equilibrium concentrations of the reaction partners (2.1) to (2.6) for the parameters $M_0 = 0.02$ mol/l, $I_0 = 0.02$ mol/l and $S_0 = 0.1$ mol/l. The total height of the figure corresponds to the total concentrations I_{tot}, M_0 respectively. For the redox potential it is equal to $1/V$.

It would be very interesting to calculate the change of concentration for the different species under illumination. This is generally not possible since we do not know the kinetic constants for all reactions to be taken into account. The back reaction

$$2\,Fe^{3+} + 3\,I^- \rightarrow 2\,Fe^{2+} + I_3^-$$

is very slow [20]. This enables to calculate – or at least to estimate – all concentrations in the photostationary state. It is assumed that in this state the reactions (2.2) to (2.6) are at equilibrium. Reaction (2.2) is diffusion controlled [17]. Our approximation should hold for the reactions (2.4) to (2.6) as well [18]. The solubility of the iodine (2.3) is more critical.

To carry out the calculations we take the equilibrium concentrations at the chosen reduction degree r as starting point. The redox equilibrium (2.1) is disturbed as a consequence of the photoinduced reaction. Therefore it has to be replaced in the calculation. The new condition can be derived from the photoinduced change in the electron distribution among iron and iodine species. The decrease of iron(II) species can be expressed by the following equation:

$$\%[\Delta Fe^{2+}] = \left| \frac{\Delta[Fe^{2+}] + \Delta[FeSO_4]}{[Fe^{2+}]_{eq} + [FeSO_4]_{eq}} \right| \cdot 100. \tag{4}$$

$[Fe^{2+}]_{eq}$ and $[FeSO_4]_{eq}$ are the equilibrium concentrations of these two species. If $2\{[I_2]_{eq} + [I_3^-]_{eq}\}$ is smaller than $\{[Fe^{2+}]_{eq} + [FeSO_4]_{eq}\}$, it is not possible to oxidize all iron(II) to iron(III). After having derived the non-equilibrium concentrations for a chosen reduction degree, it is possible to calculate the half cell potentials as follows:

$$E(Fe^{3+}/Fe^{2+}) = E^\circ_{Fe^{3+}/Fe^{2+}} + \frac{RT}{F} \ln \frac{[Fe^{3+}]}{[Fe^{2+}]}$$

$$E(I_3^-/I^-) = E^\circ_{I_3^-/I^-} + \frac{RT}{2F} \ln \frac{[I_3^-]}{[I^-]^3}$$

$$E^\circ_{Fe^{3+}/Fe^{2+}} = 0.77 \text{ V}; \quad E^\circ_{I_3^-/I^-} = 0.534 \text{ V} \quad [12].$$

The same mathematical framework for solving implicit equations can be used for the calculation of equilibrium as well as nonequilibrium concentrations [15, 19]. Calculated photostationary concentrations and half cell potentials are shown in Figure 2. They have been obtained starting from the reduction degree $r = 0.5$ in Figure 1.

The iron exists mainly as sulfato complex while the concentration of FeI^{2+} is very small at equilibrium. The nonequilibrium situation, however, is dominated by the concentrations of I^-, FeI^{2+}, and $FeSO_4^+$. The relatively small potential difference is due to the complexation of iron(III). For $\%[\Delta Fe^{2+}] = 60\%$ the potential difference is only about 100 mV.

The question arises which conditions would permit to obtain much higher potential differences. This means that the quotients $[Fe^{3+}]/[Fe^{2+}]$ and $[I^-]^3/[I_3^-]$ should increase as much as possible. Such a situation could be obtained by using a ligand X which has a different affinity to iron(II) than to iron(III). This idea can be checked by adding the following two reactions to the equilibria (2.1) to (2.6):

$$Fe^{3+} + X \rightleftarrows Fe(III)X \quad K_7 \tag{2.7}$$

$$Fe^{2+} + X \rightleftarrows Fe(II)X \quad K_8 \tag{2.8}$$

It is useful to introduce the abbreviations:

$$X_0 = [X] + [Fe(III)X] + [Fe(II)X]$$

$$k_i := K_i X_0; \quad i = 5, \ldots, 8.$$

We restrict the discussion to the situation already met in Figure 2: $M_0 = I_{tot} = 0.02$ mol/l, $S_0 = 0.1$ mol/l and $r = 0.5$. The higher k_7 and k_8, the more stable the corresponding complexes. By systematic variation of k_7 and k_8 it can be shown that the following condition is favourable for higher potential differences:

$$k_8 \gg k_7 \quad \text{and} \quad k_8 \gg k_5, k_6.$$

A plot demonstrating the influence of k_7 on the equilibrium concentrations is shown in Figure 3 for the reduction degree $r = 0.5$.

It is interesting to note that only the two iron species Fe(II)X and Fe(III)X can exist in the whole region. The nonequilibrium concentrations and the half cell potentials for the situations $k_8 = 10^5$, $k_7 = 10$ are shown in Figure 4. We conclude that it would be very interesting to find an appropriate ligand X to realize this situation.

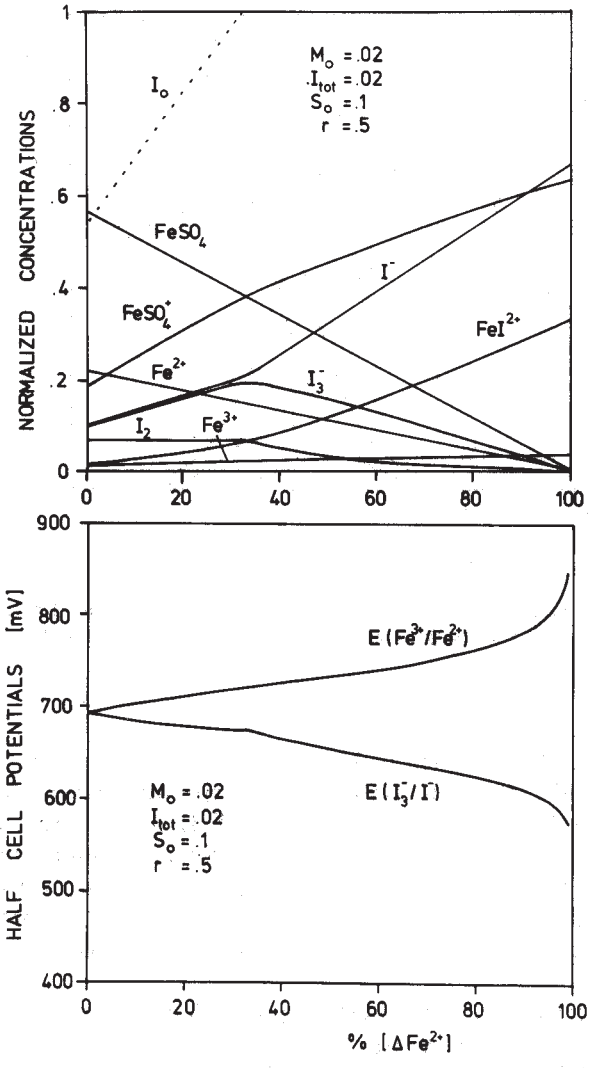

Fig. 2. Normalized concentrations and half cell potentials in photostationary states for $r = 0.5$; solution 6, Table 1. At the starting point $\%[\Delta Fe^{2+}]=0$ the concentrations and the potentials correspond to the equilibrium situation $r=0.5$ in Figure 1

3. Experimental set-up

The thermal back reaction $2Fe^{3+}+3I^- \rightleftarrows 2Fe^{2+}+I_3^-$ takes several hours [20]; see also Figures 9 and 11. It is therefore possible to separate the electrode compartment and the absorption measurement cell from the photoreactor. We have built a flow system isolated from air. The photo-

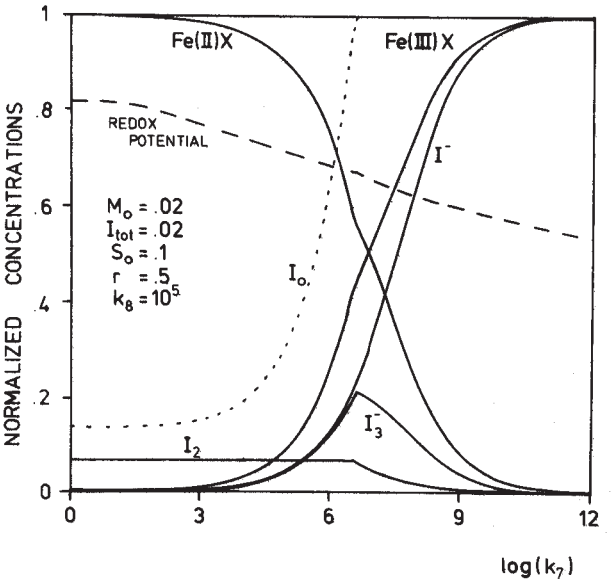

Fig. 3. Normalized equilibrium concentrations and equilibrium potential at fixed reduction degree $r=0.5$ versus the logarithm of k_7, defined in eq. (2.7), (2.9)

reactor has been thermostated to 25 °C. We have measured the following parameters (see Fig. 5): light intensity at given spectral distribution, potential of the two selective electrodes SE I and SE II versus a KCl-saturated calomel electrode, light absorption of the solution at constant wavelength, temperature on the electrode surface and electrical current between SE I and SE II at different external resistances R_L (see Fig. 9). The broad band interference filters K40, K45, K50, K55, and K60 from Balzers have been used.

The characteristics of the different optical elements have to be taken into account to make quantitative measurements available. The relative spectral distribution $V_{KX}(\lambda)$ of the photon flux for a filter KX in our arrangement is:

$$V_{KX}(\lambda) = S_{KX} \frac{L(\lambda) \cdot T_{KX}(\lambda)}{\int_{\lambda_1}^{\lambda_2} \frac{L(\lambda) \cdot T_{KX}(\lambda)}{O(\lambda)} d\lambda} \left[\frac{1}{\text{wavelength}}\right] \tag{5}$$

S_{KX} = splitting ratio of the beam splitter BS
$L(\lambda)$ = relative spectral power distribution of the light source [watt/wavelength]
$T_{KX}(\lambda)$ = transmission characteristic of the filter KX

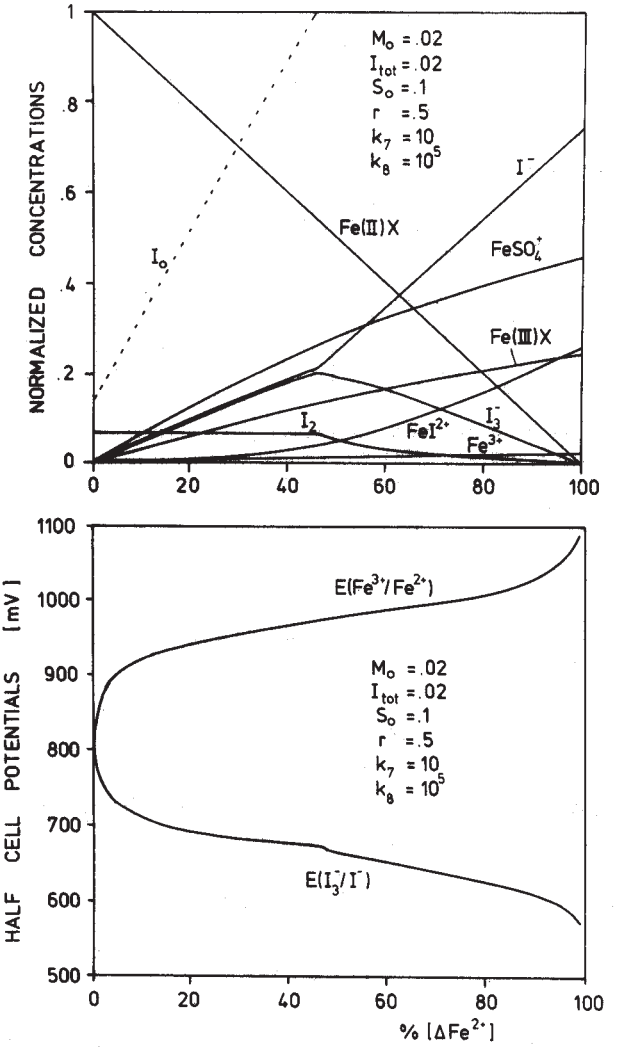

Fig. 4. Normalized concentrations and half cell potentials in photostationary states, starting from the situation $\log(k_7)=1$ in Figure 3

$O(\lambda)$ = spectral sensitivity of the power meter
N_L = Avogadro's number.

Knowing the spectral distribution $V_{KX}(\lambda)$ of the photon flux, it is easy to calculate the photocurrent $J_{KX}(\lambda)$ impending the photoreactor. The light power measured by the power meter (optometer) is called E_{Opt} [watt].

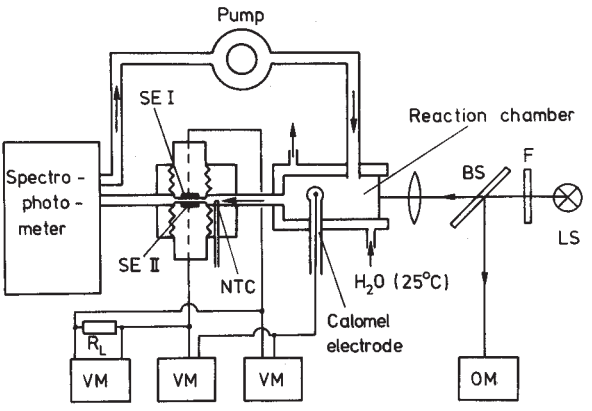

Fig. 5. Experimental set-up for the observation of photogalvanic behaviour of the iodine/iron system. LS = light source, 200 watt HBO W/2 Osram, BS = beam splitter. OM = calibrated optometer; 80X United Detector Technology Inc. VM = voltmeter. R_L external resistor. SE I and SE II = selective electrodes (SE I = glassy carbon, SE II = sintered and doped tin dioxide). F = filter

$$J_{KX}(\lambda)=\frac{E_{\mathrm{Opt}}}{(hc/\lambda)\cdot N_L}\cdot V_{KX}(\lambda)\quad[\mathrm{Einstein/(sec\cdot wavelength)}] \tag{6}$$

or

$$J_{KX}=\frac{E'_{\mathrm{Opt}}}{hc}\int_{\lambda_1}^{\lambda_2} V_{KX}(\lambda)\lambda\cdot \mathrm{d}\lambda\ . \tag{6a}$$

Since we have used broad band interference filters $\Delta\lambda\approx 50$ nm, it is necessary to define the mean wavelength $\bar{\lambda}_{KX}$ of each filter:

$$\bar{\lambda}_{KX}=:\frac{\int_{\lambda_1}^{\lambda_2} V_{KX}(\lambda)\lambda\,\mathrm{d}\lambda}{\int_{\lambda_1}^{\lambda_2} V_{KX}(\lambda)\,\mathrm{d}\lambda}\ . \tag{7}$$

The surface of the pyrex window 1 of the photoreactor shown in Figure 6 measures 1.5 cm^2. The reactor is covered with a cooling coat 2. Its length is 5.5 cm. The solution flows from 3 to 4. 5 is used for filling the system and for bubbling nitrogen gas through it. The calomel electrode is put into position 6. The PVC screw 7 is used to join the reactor and the electrode chamber.

The scheme of the electrode chamber is shown in the next figure. As building material we have used teflon. O-rings have been applied to separate the electrode chamber from the Araldit part of the electrode. The iron(II)/iron(III) selective electrode consists of n-conductive tin oxide ceramics [5, 6]. In order to produce this ceramic, 100 parts tin(IV) oxide and 2.5

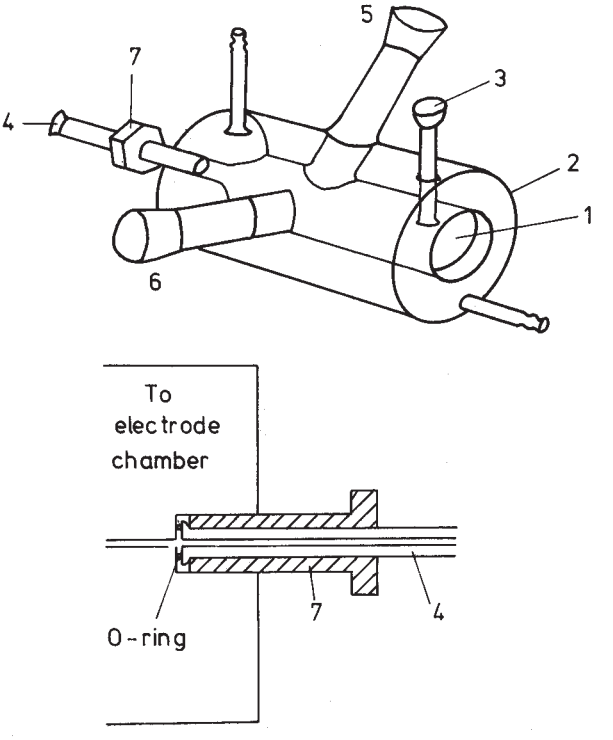

Fig. 6. Photoreactor and fixation to the electrode chamber. See text for explanation

parts antimony(III) oxide are ground, pressed into tablets and sintered during 4 hours at 1300 °C. Thus obtained ceramic is porous and therefore permeable for electrolyte. To avoid corrosion the tablet must have direct contact with an inert material and be packed into plastic. Good results are obtained with a simple technique: the tablet is pressed very strongly to the bottom of a graphite cylinder to which some Araldit has been applied. The electrode is now put into a teflon form which is carefully filled with Araldit (100 parts of Araldit D+9 parts of "Härter" HY931). The electrode is polished with a suspension of Al_2O_3 in water.

4. Quantum yield

Although the individual concentrations of I_3^- and I_2 can be determined by spectrophotometric measurements, the experimental information is to be handled carefully. The spectra of I_3^- and I_2 shown in Figure 8 have been obtained by a method described by Awtrey and Connick [21]. The ions Fe^{3+}, I^-, and Fe^{2+} do not absorb any light below 410 nm.

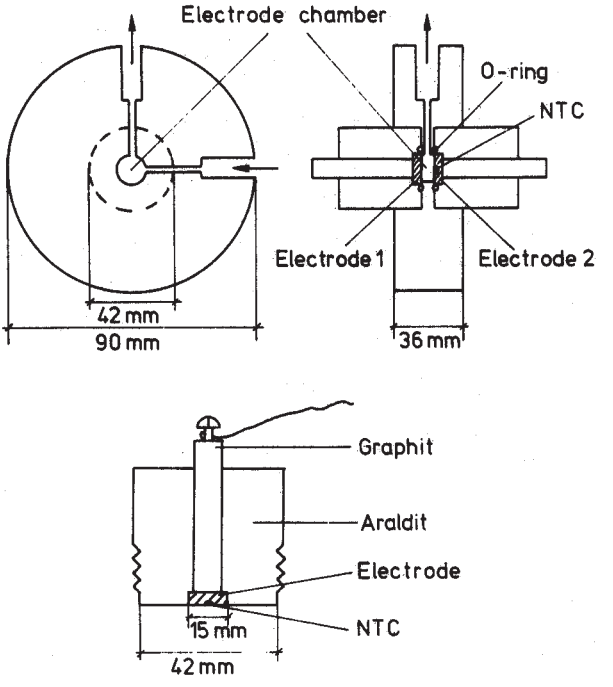

Fig. 7. Longitudinal and cross section of the electrode chamber and the electrode. The distance between the two electrodes is 5 mm. Electrode 1 is glassy carbon, Type 452 – 10.311, V 10 from Le Carbone Lorraine. Electrode 2 is doped and sintered tin dioxide

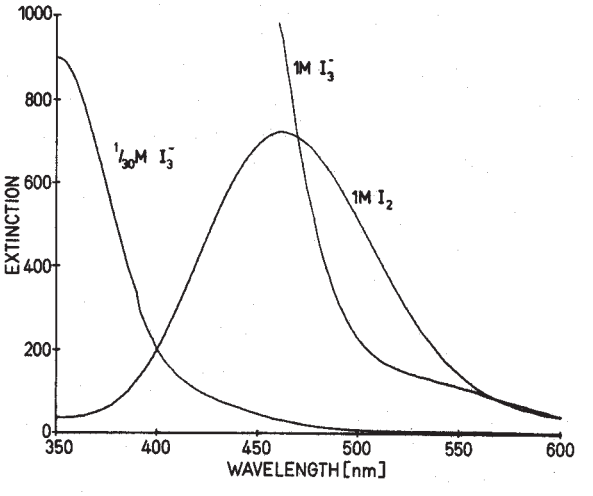

Fig. 8. Absorption spectra of I_2 and I_3^- at 25 °C. Path length 1 cm

Knowing the relative spectral distribution of the photon flux $J_{KX}(\lambda)$ (6) as well as the extinction coefficients $\varepsilon_{I_2}(\lambda)$, $\varepsilon_{I_3^-}(\lambda)$ and the concentration $\{[I_2]+[I_3^-]\}$, the number of photons/s $J_A(t)$ absorbed are:

$$J_A(t)=\int_{\lambda_1}^{\lambda_2} J_{KX}(\lambda)Q(\lambda, t)\mathrm{d}\lambda. \tag{8}$$

$Q(\lambda, t)$ is the fraction of light absorbed by the solution:

$$Q(\lambda, t)=\frac{I_0-I(t)}{I_0}(\lambda)=1-10^{-A(\lambda,t)} \tag{9}$$

$$A(\lambda, t)=d\cdot\sum_i \varepsilon_i(\lambda)C_i(t)$$

d = cell length (5.5 cm)
$C_i(t)$ = individual concentrations [Mol/l]
$\varepsilon_i(\lambda)$ = individual extinction coefficients [cm²/Mol].

Out of the equations (6), (8), and (9) we get:

$$J_A(t)=\frac{E'_{Opt}}{hc}\int_{\lambda_1}^{\lambda_2} V_{KX}(\lambda)\lambda(1-10^{-d\{\varepsilon_{I_2}(\lambda)[I_2]+\varepsilon_{I_3^-}(\lambda)[I_3^-]\}})\mathrm{d}\lambda. \tag{10}$$

We do not know if excited I_2 or I_3^- is the active species in the electron-transfer-reaction with iron(II), although there exist some investigations on the subject in aqueous solution [16a, 22]. As can be derived from the results in section 2 this problem is not easy to solve. The best thing is therefore to assume that both I_2 and I_3^- are photoactive. This leads to an overall quantum yield Φ which is defined as quotient between photons absorbed J_A by the solution and iron(II) species J_e oxidized at the same time:

$$\Phi=\frac{J_A}{J_e}. \tag{11}$$

C is the abbreviation for the total concentration of I_2 and I_3^- species:

$$C=[I_2]+[I_3^-]. \tag{12}$$

Its change $\dot{C}=\frac{\mathrm{d}C}{\mathrm{d}t}$ in relation to time is:

$$\dot{C}=-\frac{\Phi\cdot J_A}{2V}+\dot{C}_b. \tag{13}$$

V is the total volume of the solution and $\dot{C}_b$ describes the thermal back reaction. Two electrons are consumed for each I_2 or I_3^- which is reduced. The factor 2 introduced in equation (13) resp. (14) is a result of this.

$$\Phi=\frac{2V}{J_A}(\dot{C}_b-\dot{C}). \tag{14}$$

To derive the necessary information from the absorbance measurements, $\dot{C}$ and $\dot{C}_b$ have to be substituted by $\dot{A}(\lambda, t)$.

Using the abbreviations

$$I_1=[I^-],\ I_F=[FeI^{2+}],\ I_1^{tot}=I_1+I_F,\ I_2=[I_2],\ I_3=[I_3^-]$$

and inserting them into the equation (14), we get:

$$\Phi=\frac{2V}{J_A}(\dot{I}_{2_b}+\dot{I}_{3_b}-\dot{I}_2-\dot{I}_3). \tag{15}$$

The following equations may be used to calculate $\dot{I}_2$ and $\dot{I}_3$ if all iodine is solved:

$$\dot{A}(\lambda, t)=\varepsilon_{I_2}(\lambda)\dot{I}_2+\varepsilon_{I_3}(\lambda)\dot{I}_3 \quad (d=1\text{ cm})$$

$$\dot{I}_0 \quad =3\dot{I}_3+2\dot{I}_2+\dot{I}_1+\dot{I}_F=0 \tag{16}$$

$$\dot{K}_2 \quad =\dot{I}_3-K_2I_1\dot{I}_2-K_2I_2\dot{I}_1=0 \tag{17}$$

$$\dot{I}_2+\dot{I}_3 \ =\dot{A}(\lambda, t)\frac{1}{\varepsilon_{I_3}(\lambda)[q+1]}+\dot{I}_F\frac{K_2}{1+3K_2I_2}\cdot\left[\frac{q}{q+1}\right] \tag{17a}$$

$$q=\frac{\varepsilon_{I_2}(\lambda)/\varepsilon_{I_3}(\lambda)-1}{1+\dfrac{K_2}{1+3K_2I_2}(I_1-2I_2)}$$

I_3 and I_2 are determined by simultaneous measurement of absorption at two different wavelengths. $\dot{A}(\lambda, t)$ is obtained by graphic derivation of the recorded function $A(\lambda, t)$ at the start of the photoreaction. Near the equilibrium C_b is much smaller than C so that Φ can be approximated by

$$\Phi_{\text{near eq.}}\approx-\frac{2V}{J_A}(\dot{I}_2+\dot{I}_3). \tag{18}$$

5. Experimental results

Typical experimental curves are shown in Figure 9A and B. Irradiation starts at the points "start" and stops at the points "stop". The upper curves demonstrate the change of light absorption at 490 nm. The lower curves visualize the change of potential of each selective electrode compared to normal hydrogen electrode. $E(Fe^{3+}/Fe^{2+})$ is observed on doped and sintered tin oxide and $E(I_3^-/I^-)$ on glassy carbon. At the point "current" different external resistances R_L have been introduced; compare Figure 5. Solution 6 (B; see Table 1) is oversaturated. The extinction at the beginning of the experiment has therefore not been constant. Systems in which not all I_2 is solved at equilibrium seem to be the most interesting for solar energy conversion, but they are difficult to understand.

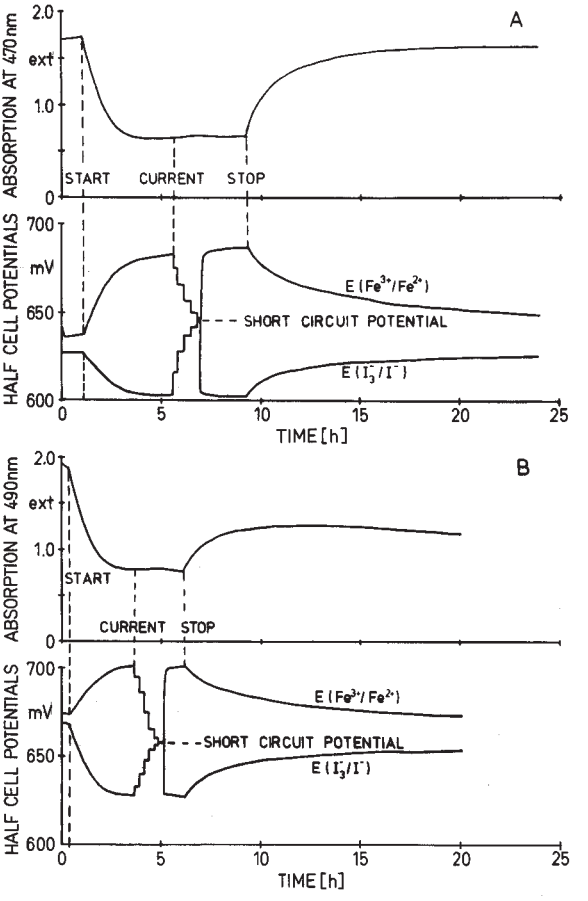

Fig. 9. Observed light absorption and half cell potentials versus time for the solutions 4 (A) and 6 (B), Table 1

The observed short circuit potential is not equal to the equilibrium potential. This is due to polarization phenomena [23], [24] which have not yet been studied in relation to this system. The light absorption is not influenced by the current. This means that even at short circuit conditions the concentrations of the photochemically produced species in our system are not influenced by the electrical current flow. This is because the electrode surface of 1.5 cm^2 is very small compared to the volume. Current-voltage and power-voltage curves for three solutions with equal total concentrations M_0, I_{tot}, and S_0 but with different reduction degree are shown in Figure 10. Table 1 reports the main experimental results from 13 different solutions irradiated at $\bar{\lambda}=447$ nm. All quantum yields have been determined at the

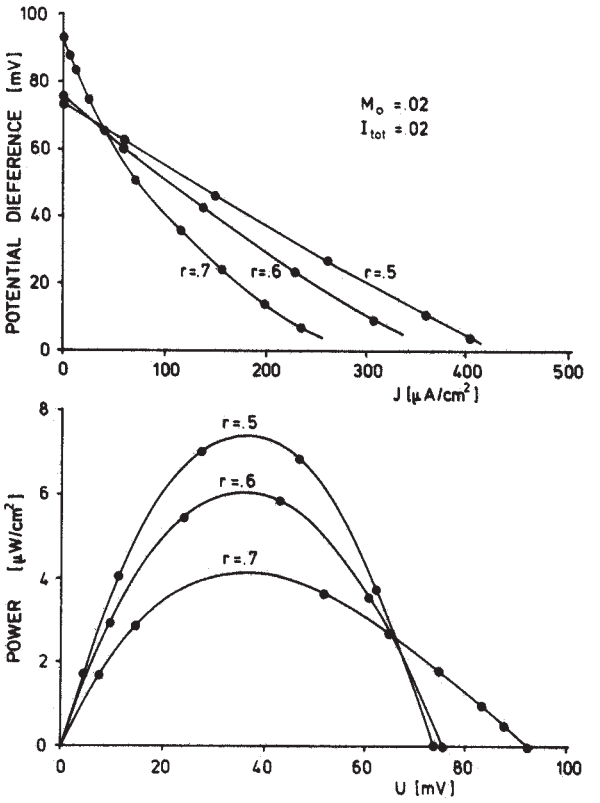

Fig. 10. Voltage current and power voltage curves for the solutions 6, 7, and 8; see Table 1

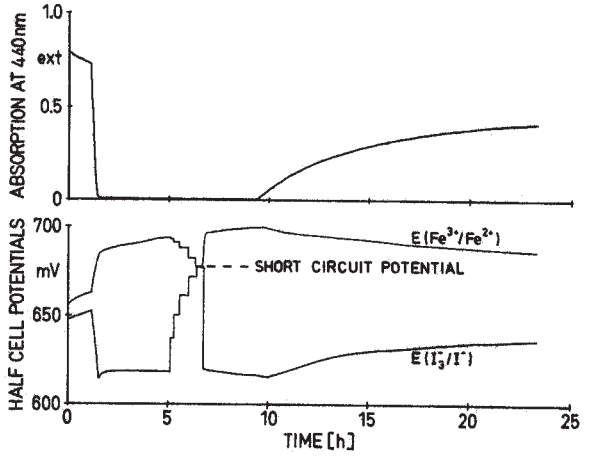

Fig. 11. The same as in Figure 9 for solution 1

Table 1. *Experimental values observed at $\bar{\lambda}=447$ nm. J_A is the light flux which has been applied, see eq. (8). U_0 is the opten circuit potential difference in the photostationary state (cf. Fig. 9); P_{max} the electrical power (cf. Fig. 10) and η is equal to P_{max} divided by the incident light power. For the quantum yield Φ see eq. (11) and (18)*

Sample	M_0 [Mol/l]	I_{tot} [Mol/l]	r	Φ	$J_A \cdot 10^6$ $\left[\frac{\text{Einstein}}{\text{ls}}\right]$	U_0 [mV]	P_{max} [μW/cm^2]	$\eta \cdot 10^3$ [%]
1	0.005	0.005	0.7		8.4	74	0.4	0.42
2	0.01	0.01	0.7		8.5	92	1.1	1.1
3	0.01	0.02	0.6	0.24	9.8	80	5.8	5.3
4	0.01	0.02	0.9	0.18	10.2	79	4.3	4.1
5	0.02	0.01	0.8	0.05	10.0	74	4.6	4.0
6	0.02	0.02	0.5	0.58	9.5	74	7.5	6.7
7	0.02	0.02	0.6	0.48	9.7	76	6.1	5.3
8	0.02	0.02	0.7	0.54	11.2	95	4.1	3.1
9	0.02	0.02	0.8	0.27	9.7	80	2.9	2.5
10	0.02	0.02	0.9	0.16	10.3	70	3.8	3.1
11	0.02	0.04	0.9	0.32	9.8	75	3.1	2.9
12	0.03	0.03	0.7	0.5	9.3	65	4.1	4.4
13	0.05	0.05	0.7	0.15	10.5	35	3.3	2.9

Table 2. *Experimental data for solution 12. Compare Table 1*

$\bar{\lambda}$ [nm]	Φ	$J_A \cdot 10^6$ [Einstein/l · s]	U_0 [mV]
404	0.29	14.5	59
447	0.5	9.3	65
486	0.48	4.5	42
561	0.26	9.1	49

beginning of each experiment. They are not the same in the different solutions. For solution 12 quantum yields have been determined at 4 different wavelengths; Table 2. There seems to be a maximum in the region of 447 nm to 486 nm. No general conclusion should be made, however, since this could vary from one solution to another.

It may be interesting to note that an extremely small back reaction has been observed in solution 1. Overshooting of the I_3^-/I^- potential took place even with the low light intensity used. This overshooting might be due to the relatively slow reaction (2.4): $Fe^{3+} + I^- \rightleftarrows FeI^{2+}$. The result of this experiment is shown in Figure 11.

The method described in section 2 enables a comparison between the calculated half cell potentials and the observed ones. Quantitative agreement cannot be expected since the activity coefficients have not been considered and since the selectivity of the electrodes is perhaps not 100%. Nevertheless at least qualitative agreement between calculated and measured curves

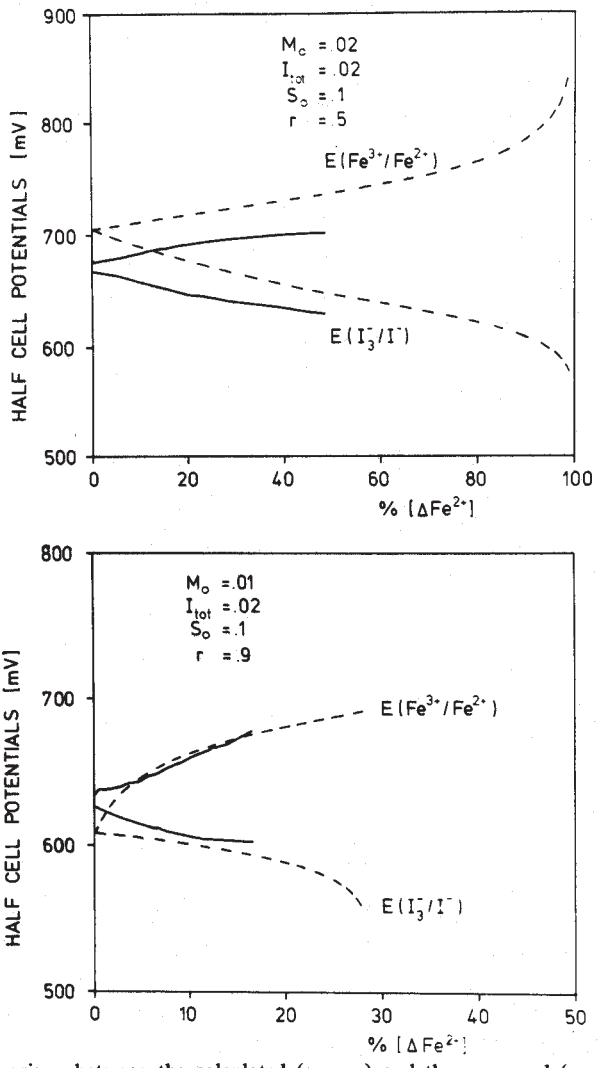

Fig. 12. Comparison between the calculated (------) and the measured (———) half cell potentials for the solutions 4 and 6, Table 1

should be observed. The two typical results shown in Figure 12 demonstrate that this is the case.

6. Conclusions

The iodine/iron photoredox system is much more complex than has been assumed up to now. Using the reduction degree as important degree

of freedom, it is possible to derive a phenomenological description of the iodine/iron photoredox system. This phenomenological description provides a good starting point for a more detailed investigation so that it might become possible to understand the primary photoprocess. We have estimated that with an appropriate reaction chamber it will be possible to transform up to 0.3% solar energy into electrical energy at full illumination [19a].

Although this is much more than any other known photogalvanic cell can achieve, it is still too low for practical application. If higher photopotentials can be obtained after an appropriate change of the system (compare Fig. 4) it will become interesting to reinvestigate its possibilities for solar energy conversion. We do not yet understand the mechanism of the selectivity of the doped tin dioxide electrode. The ideas described by Gerischer [25], however, provide the necessary theoretical background. But it seems that specific interactions between the iron ions and the tin(IV) oxide surface have to be taken into account [11].

Acknowledgement

This paper is part of project No. 4.099–0.76.04 of the Swiss National Science Foundation. We thank Prof. Dr. E. Schumacher for support of this work.

References

1. E. K. Rideal and E. G. Williams, J. chem. Soc. **127** (1925) 258.
2. T. Ohta, S. Asakura, M. Yamaguchi, N. Kamiya, N. Gotoh, and T. Otagawa, Intern. J. of Hydrogen Energy **1** (1976) 113.
3. Specialist Periodical Reports, The Chemical Society; Photochemistry, Vol. 6, Part V, 1975
4. G. Calzaferri, Chimia **32** (1978) 241.
5. G. Calzaferri and H. R. Grüniger, Helv. **61** (1978) 950.
6. H. R. Grüniger, J. Baumann, and G. Calzaferri, *Selective Electrode Material for the Iron Ions Fe^{3+}/Fe^{2+} in the Iron/Iodine System.* Extended Abstract of the 2nd Int. Conf. on the Photochemical Conversion and Storage of Solar Energy, Cambridge, 10.8.–12.8.1978, p. 53
7. G. Calzaferri and Th. Dubler, Ber. Bunsenges. Phys. Chem. **76** (1972) 1143.
8. G. Calzaferri and H. R. Grüniger, Z. Naturforsch. **32a** (1977) 1036.
9. L. Michaelis, Chem. Rev. **16** (1935) 243.
10. G. Calzaferri and J. Baumann, Z. Phys. Chem. Neue Folge, in press.
11. H. R. Grüniger, Ph. D. thesis, University of Bern, Institute for Inorganic and Physical Chemistry, July 1979.
12. CRC-Handbook of Chemistry and Physics. 53rd Ed. 1972/73.
13. Stability Constants; The Chemical Society London; Special Publication No. 17 (1964) and Supplement No. 1, Special Publication No. 25 (1971). – G. Jones and B. B. Kaplan, J. Am. Chem. Soc. **50** (1928) 1845. – A. I. Popov, in: *Halogen Chemistry*, Vol. 1, Ed. V. Gutmann. Academic Press, 1967.
14. *Ullmanns Enzyklopädie der Techn. Chemie.* Urban & Schwarzenberg, München 1957. Band 9, 3. Aufl., p. 124.
15. Th. Dubler, C. Maissen, and G. Calzaferri, Z. Naturforsch. **31b** (1976) 569.

16. T. L. Allen and R. M. Keefer, J. Am. Chem. Soc. **77** (1955) 2957.
16a. A. Barkatt and M. Ottolenghi. Mol. Photochem. **6** (1974) 253.
17. O. E. Myers, J. Chem. Phys. **28** (1958) 1027.
18. F. Basolo and R. Pearson, *Mechanismen in der anorganischen Chemie*, Georg Thieme Verlag, Stuttgart 1973, p. 165.
19. F. Erwe, *Differential- und Integral-Rechnung I*, Chapter V.5, BI-Hochschultaschenbücher, 30/30a, 1964.
19a. J. Baumann, diploma thesis, University of Bern, Institute for Inorganic and Physical Chemistry, 1979.
20. N. Sasaki, Z. Anorg. Chem. **122** (1922) 61.
21. A. D. Awtrey and R. E. Connick, J. Am. Chem. Soc. **73** (1951) 1842.
22. J. C. Roy, W. H. Hamill and R. R. Williams, J. Am. Chem. Soc. **77** (1955) 2953.
23. K. J. Vetter, *Elektrochemische Kinetik*. Springer-Verlag, Berlin 1961.
24. W. J. Albery and A. W. Foulds, J. Photochem. **10** (1979) 41.
25. H. Gerischer, Z. Phys. Chem. Neue Folge **27** (1961) 48. – H. Gerischer, in: *Physical Chemistry, An Advanced Treatise*. Vol. IXA, Academic Press, New York 1970.